

## Supporting Information

### **Molecular Weight Dependence of the Morphology in P3HT: PCBM Solar Cells**

*Feng Liu, Dian Chen, Cheng Wang, Kaiyuan Luo, Weiyin Gu, Alejandro L. Briseno, Julia*

*W. P. Hsu and Thomas P. Russell\**

Dr. F. Liu, D. Chen, W. Gu, Prof. A. L. Briseno, Prof. T. P. Russell

Department of Polymer Science and Engineering, University of Massachusetts, Amherst,  
Massachusetts 01003, United States

E-mail: tom.p.russell@gmail.com

Dr. C. Wang

Advanced Light Source, Lawrence Berkeley National Laboratory, Berkeley, California  
94720, United States

K. Luo, Prof. J. W. P. Hsu

Department of Materials Science and Engineering, University of Texas at Dallas,  
Richardson, TX 75080

Photoelectron emission spectroscopy in air (PESA) uses a monochromatized UV light to excite photoelectrons from the sample surface. The emitted electrons are accelerated by a weak electric field applied between the sample and the suppresser grid. The electrons become attached to oxygen molecules to form  $O_2^-$  ions, which are accelerated again by a strong field applied between the quenching grid and anode. In this process, the electrons are detached from the oxygen molecules through an electron cascading process and are then detected. Plotting the yield of photoelectrons as a function of the energy of the UV light, there is a clear threshold above which the number of photoelectrons generated is clearly above the background level. The threshold energy in the PESA measurement corresponds to the ionization potential, i.e. Fermi level in metals and highest occupied molecular orbital (HOMO) in organic materials. PESA has been used to study metals, organic materials, and semiconductor nanocrystals. We performed PESA on thin films under constant dry air flow using a Riken Keiki AC-2 spectrometer. In contrast to cyclic voltammetry, which provides information on the electronic properties of an isolated molecule, PESA measures the electronic properties of the molecules after forming a thin film, hence including the effect of packing between neighboring molecules that is strongly influenced by the interaction of side/end groups. Hence PESA results are more suitable for corroborating with device results.

Melting point depression experiment was carried out to evaluate interaction parameter  $\chi$  between P3HT and PCBM. The samples were prepared by adding a little amount of PCBM into P3HT (usually 2-20 wt %). These blended samples were dissolved in chloroform and then drop casted to DSC pan. Then use DSC to check the

melting point change. The samples were firstly heated at a rate of 10 °C/min to 280 °C and held for 5 minutes. Subsequently the samples were cooled to 0 °C at 2 °C/min and held for 5 minutes. Then the samples were heated again at a rate of 10 °C/min to 280 °C, and the melting point ( $T_m$ ) was obtained from the high temperature side intersection of the base line with the tangent to the endotherm.  $T_m^0$  is the melting point of the pure P3HT obtained using the same procedure. Detailed data see Figure S5.

In GIWAXS, the diffraction pattern for semicrystalline polymers usually shows arcs with an azimuthal angle intensity distribution. A quantitative analysis of these arcs can provide us information on crystallites and chain orientation of the polymers. This is because the scattered intensity at a given angle to the meridian is related to the number of crystallites inclined at the same angle to the orientation direction. In this work, we studied crystallite orientation by quantitatively measuring normalized orientation distribution functions (ODF) of (100) crystallographic axes. The normalized orientation distribution functions of reciprocal lattice vectors and their second moments were determined by quantitative GIWAXS. The second moments of ODF is determined by equation S1 and orientation factor is calculated by equation S2.

$$\langle \cos^2 \varphi \rangle = \frac{\int_0^{\pi/2} H(\varphi) \cos^2 \varphi \sin \varphi d\varphi}{\int_0^{\pi/2} H(\varphi) \sin \varphi d\varphi} \quad (S1)$$

$$f_{hkl} = \frac{1}{2} \left( 3 \langle \cos^2 \varphi \rangle - 1 \right) \quad (\text{S2})$$

In which  $H(\varphi)$  is ODF,  $\varphi$  is the azimuthal angle.

For those samples denoted as “Pre-Annealed”, the active layer was annealed at the specified temperature for the specified time and then the Al cathode was evaporated onto the surface. For those samples denoted as “Post-Annealed”, the Al cathode was first evaporated onto the active layer and then annealed.

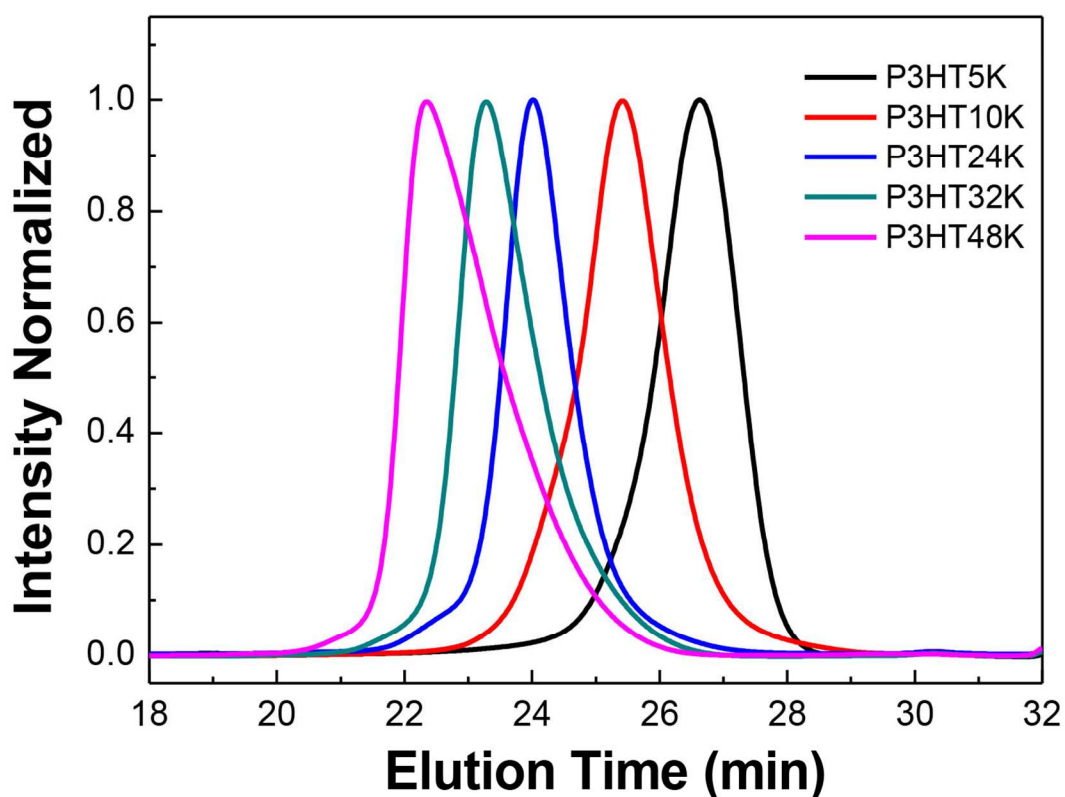


**Figure S1.** GPC traces of synthesized P3HTs using Chloroform as eluent.

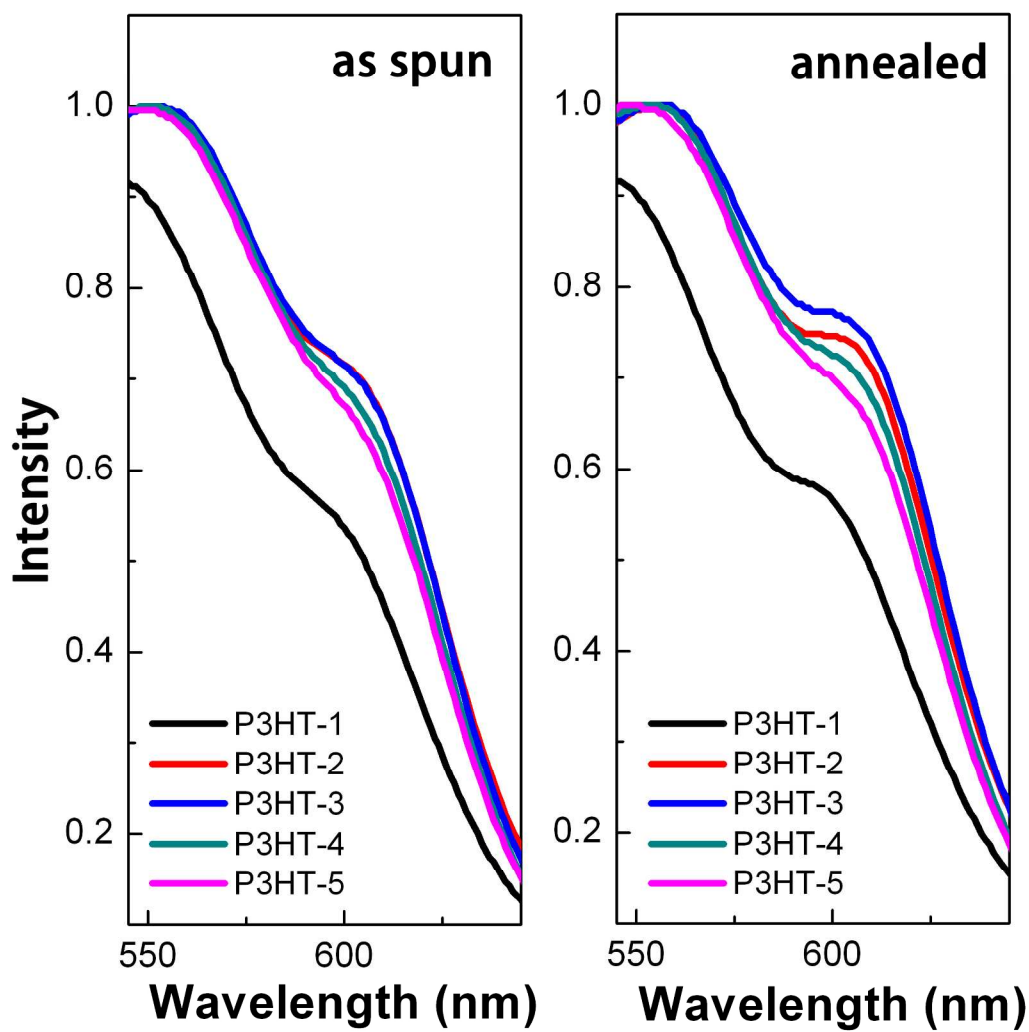


**Figure S2.** Comparison of UV-vis absorption of P3HT samples before and after thermal annealing.

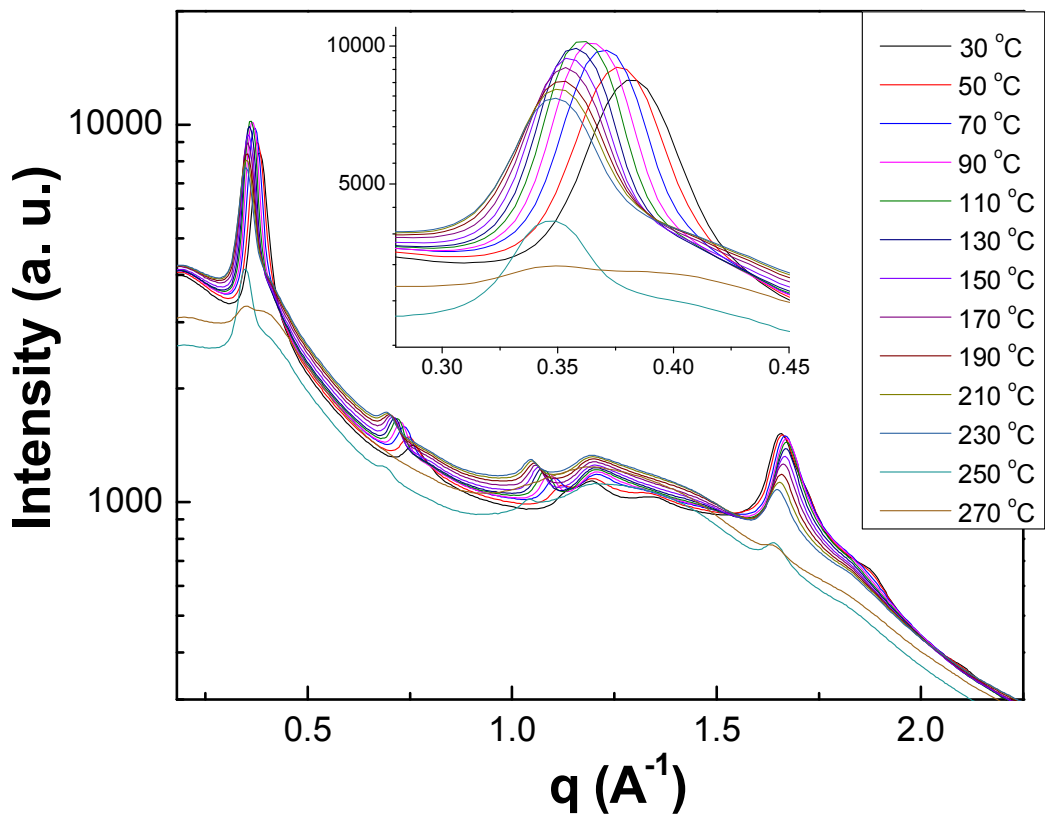


Figure S3. Typical In-Situ XRD results of P3HT samples under thermal annealing.

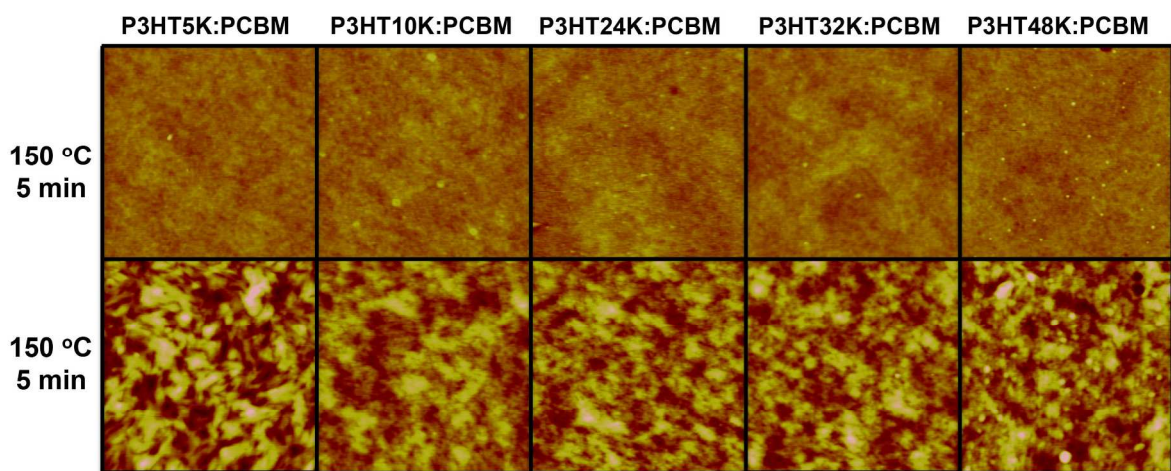
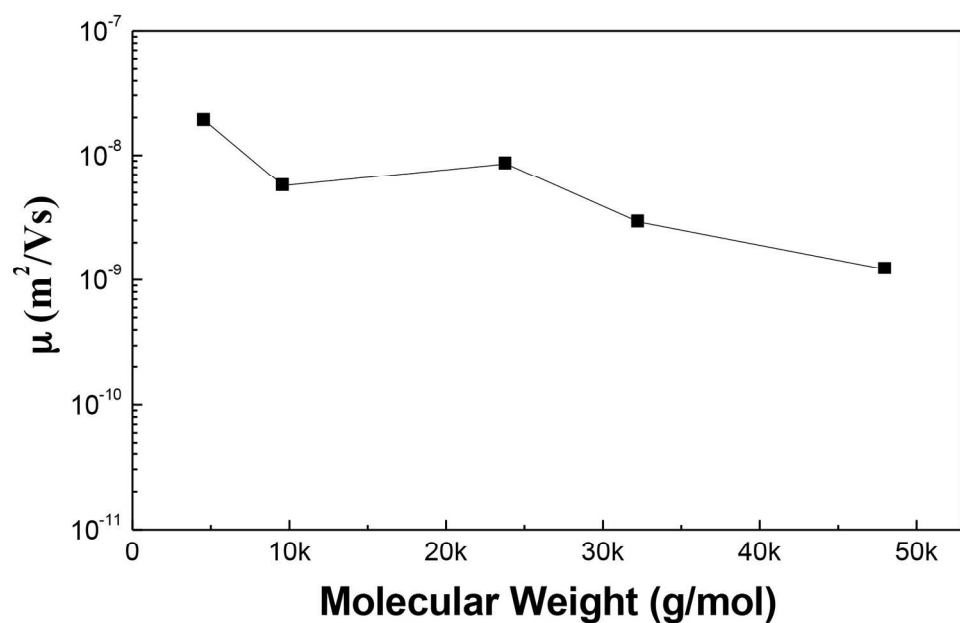
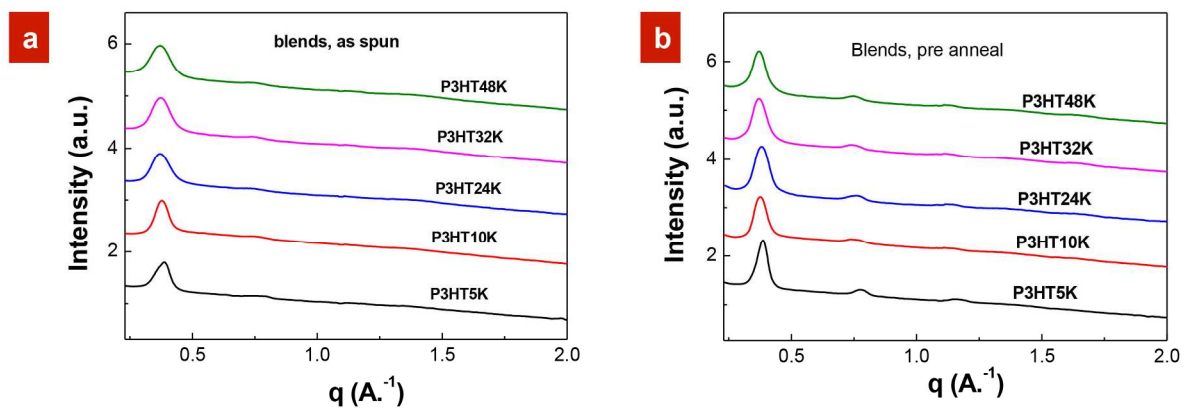


Figure S4. SPM images of pre-annealed and post-annealed P3HT:PCBM blends.



**Figure S5.** SCLC hole mobility of post-annealed P3HT:PCBM blends using ITO/PEDOT:PSS/Active layer/Au single carrier devices.



**Figure S6.** GIXD of as spun (a) and pre-annealed (b) P3HT:PCBM blends.

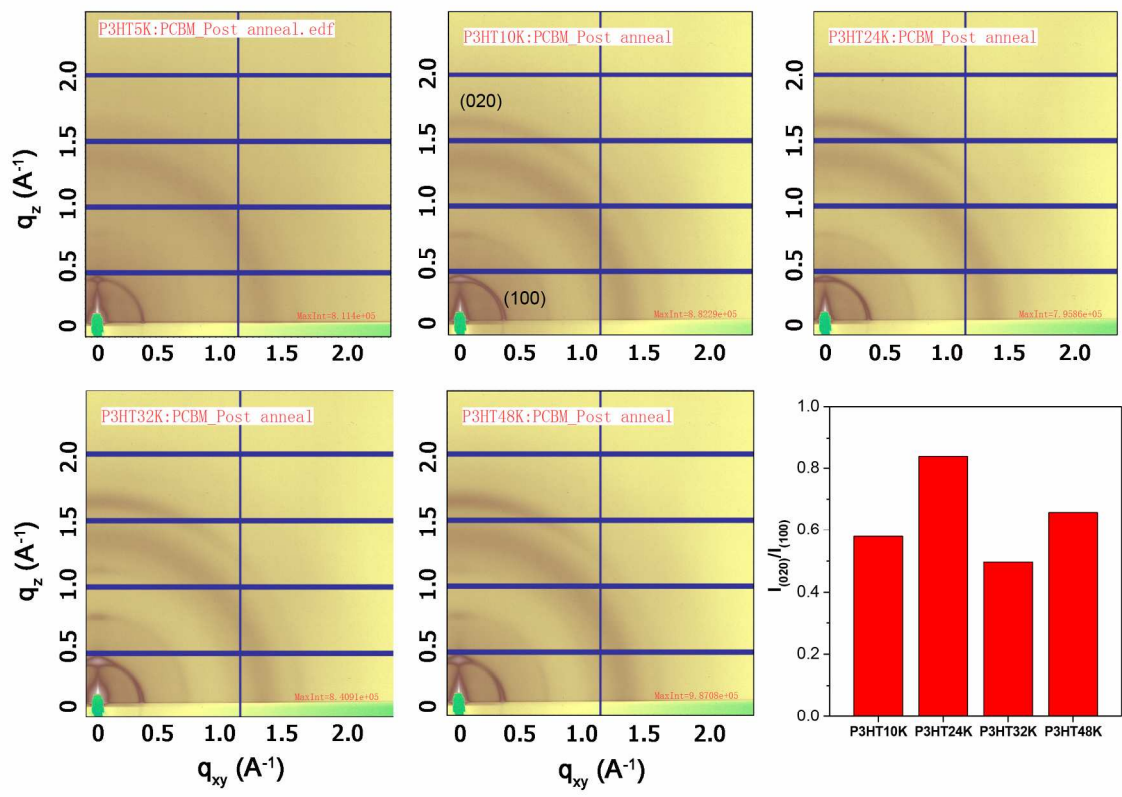


**Figure S7.** GIXD image of post-annealed P3HT:PCBM blends and the (020) peak to (100) peak intensity ratio.

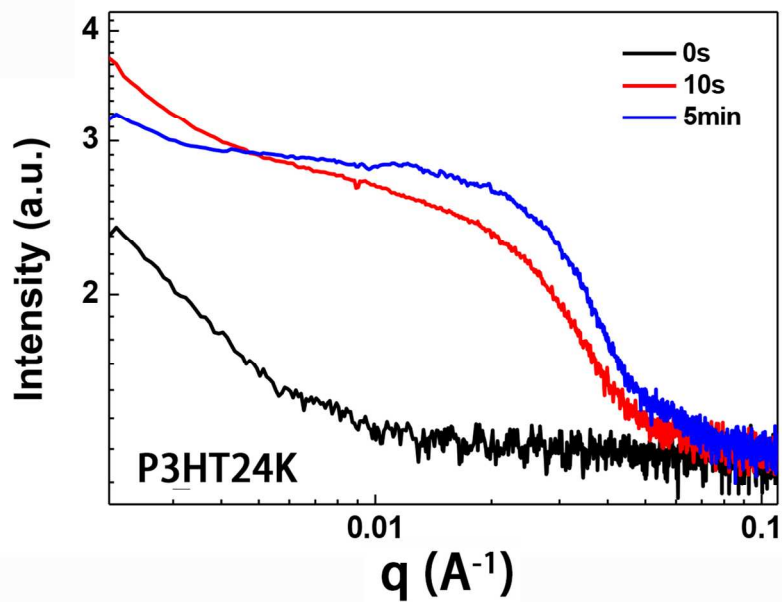


**Figure S8.** GISAXS of P3HT:PCBM blends under different thermal annealing time.